Immobilization of Bis(imino)pyridyliron(II) Complexes on Silica

Franz A. R. Kaul, Gerd T. Puchta, Horst Schneider, Frank Bielert, Dimitrios Mihalios, and Wolfgang A. Herrmann*

Anorganisch-chemisches Institut der Technischen Universität München, Lichtenbergstrasse 4, D-85747 Garching, Germany

Received November 3, 2000

The well-known catalyst precursor 2,6-bis[1-((2,6-diisopropylphenyl)imino)ethyl]pyridine (**1**) is functionalized by various alkenyl groups to yield the corresponding alkenyl-functionalized 2,6-bis[1-((2,6-diisopropylphenyl)imino)ethyl]pyridine ligand. Reaction of these novel functionalized bis(imino)pyridyl ligands with iron(II) chloride results in the formation of precatalysts **5**−**7**, which possess different spacer moieties. The possibility of self-immobilization has been investigated with respect to the chain length of the alkenyl moiety. Additionally, experiments to heterogenize these functionalized iron(II) complexes on modified silica via hydrosilation are presented (**8**−**10**). The immobilization has been studied by IR, and the resulting polymers have been characterized by GPC and static light scattering.

Introduction

Since the discovery of Brookhart[1] and Gibson[2] that complexes of late transition metals such as iron and cobalt are capable of polymerizing α-olefins, the interest in polymerization catalysts other than metallocenes has greatly increased. Because of their lower oxophilicity,[3] these "post-metallocene catalysts" are well-suited for application in the copolymerization of α-olefins with polar monomers such as alkyl acrylates.[3,4] Due to problems (e.g. reactor fouling and an extremely exothermic polymerization process) arising from the homogeneous nature of the polymerization catalysts, the application of these polymerization catalysts in gas-phase or slurry reactions still is comparatively problematic. Up to now, use of the [bis(imino)pyridyl]iron(II) complexes in a continuous process has been difficult, as the polyolefins produced will deposit at the reactor walls and the stirring device, a problem which might be overcome by tailoring the polymer morphology via heterogenization of the homogeneous compounds.

Most often, inorganic support materials such as silica or alumina,[5] and also organic supports such as polystyrene and starch,[6] have been used to heterogenize soluble polymerization catalysts. A different heterogenization strategy was applied by Alt et al., who provided metallocenes with alkene functionalities and used these functionalized metallocenes as comonomers in the polymerization process.[7] To the best of our knowledge, there have been no experiments to apply the latter heterogenization techniques to late-transition-metal catalysts.

Herein we report the versatile heterogenization technique to immobilize [2,6-bis[1-(2,6-(diisopropylphenyl)-imino)ethyl]pyridyl]iron(II) chloride, which exhibits excellent activity in olefin polymerization after activation with MAO or MMAO but severely suffers from the insolubility of the produced polymers, resulting in a dramatic reactor fouling during the polymerization process.

Experimental Section

General Considerations. All experiments were carried out under an atmosphere of dry, purified nitrogen or argon using glovebox or standard Schlenk techniques. All solvents were dried and deoxygenated as described in ref 8 and kept under argon and molecular sieves (4 Å). NMR spectra were recorded on JEOL JNM GX-400 and Bruker DPX-400 instruments. The solvent signals were used for internal calibration. All spectra were obtained at room temperature unless otherwise stated. Polymer samples were dissolved in a mixture of 1,2,4-trichlorobenzene and $C_2D_2Cl_4$ and analyzed via NMR spectroscopy at a temperature of 120 °C. Elemental analyses were performed in the microanalytical laboratory of our institute.

The obtained polymers were analyzed using a combination of a Waters 150 CV high-temperature GPC at 135 °C with 1,2,4-trichlorobenzene as solvent and a modified Whyatt Minidawn light-scattering instrument. The calibration was performed with polystyrene standards and conversion into PE and PP calibration curves using Mark−Houwink parameters.

(1) (a) Small, B. L.; Brookhart, M.; Bennett, A. M. A. *J. Am. Chem. Soc.* **1998**, *120*, 4049−4050. (b) Small, B. L.; Brookhart, M. *J. Am. Chem. Soc.* **1998**, *120*, 7143−7144.

(2) (a) Britovsek, G. J. P.; Gibson, V. C.; Kimberley, B. S.; Maddox, P. J.; McTavish, S. J.; Solan, G. A.; White, A. J. P.; Williams, D. J. *Chem. Commun.* **1998**, 849−850. (b) Britovsek, G. J. P.; Gibson, V. C.; Kimberley, B. S.; Maddox, P. J.; McTavish, S. J.; Solan, G. A.; White, A. J. P.; Williams, D. J.; Bruce, M.; Mastroianni, S.; Redshaw, C.; Strömberg, S. *J. Am. Chem. Soc.* **1999**, *121*, 8728−8740. (c) Britovsek, G. J. P.; Gibson, V. C.; Wass, D. F. *Angew. Chem.* **1999**, *111*, 448−468; *Angew. Chem., Int. Ed.* **1999**, *38*, 428−447.

(3) Johnson, L. K.; Mecking, S.; Brookhart, M. *J. Am. Chem. Soc.* **1996**, *118*, 267−268.

(4) Younkin, T. R.; Connor, E. F.; Henderson, J. I.; Friedrich, S. K.; Grubbs, R. H.; Bansleben, D. A. *Science* **2000**, *287*, 460−462.

(5) (a) Jackson, R.; Ruddlesden, J.; Thompson, D. J.; Whelan, R. *J. Organomet. Chem.* **1977**, *125*, 57−62. (b) Kaminsky, W. *Macromol. Chem. Phys.* **1996**, *197*, 3907−3945 and references therein.

(6) Boussie, T. R.; Coutard, C.; Turner, H.; Murphy, V.; Powers, T. S.; *Angew. Chem.* **1998**, *110*, 3472−3475.

(7) Alt, H. G. *J. Chem. Soc., Dalton Trans.* **1999**, 1703−1709.

(8) Pangborn, A. B.; Giradello, M. A.; Grubbs, R. H.; Rosen, R. K.; Timmers, F. J. *Organometallics* **1996**, *15*, 1518−1520.

10.1021/om000939t CCC: $22.00 © 2002 American Chemical Society
Publication on Web 12/05/2001

The infrared spectra of the homogeneous compounds were recorded on a Perkin-Elmer 1600 FT-IR instrument as KBr pellets. The supported precatalyst samples were prepared under an inert atmosphere as self-supporting pellets and analyzed using NaCl windows. All BET surface determinations and BJH pore-size distributions were carried out using a Micromeritics ASAP 2000 nitrogen porosimeter.

Allyl bromide, 4-bromo-1-butene, 5-bromo-1-pentene, and lithium diisopropylamide (2 M in toluene) were purchased from Aldrich Chemicals and were used without further purification. The "Karstedt catalyst" (platinum−divinyltetramethyldisiloxane complex in vinyl-terminated poly(dimethylsiloxane)) was obtained from ABCR and used as received.

As a support, silica (Aeroperl 300/40, Degussa-Hüls AG) with a BET surface area of 300 m^2/g, a pore volume of 1.9 cm^3/g, and a main particle size of 40−120 μm was used. Co−methylaluminoxane (Witco, 10% in heptane) was used as cocatalyst. Ethene (AGA Gas GmbH, grade 3.5) and propene (Linde AG, grade 2.8) were purified by passing them through two purification columns containing activated BTS catalyst and molecular sieves (4 Å) before feeding the reactor.

Synthesis of 2-[1-(2,6-(Diisopropylphenyl)imino)ethyl]-6-[1-(2,6-(diisopropylphenyl)imino)-4-pentenyl]pyridine (2). To a vigorously stirred solution of 2 g (4.15 mmol) of 2,6-bis[1-(2,6-(diisopropylphenyl)imino)ethyl]pyridine (**1**) in 60 mL of absolute THF was added 2.2 mL (1.05 equiv) of lithium diisopropylamide (2 M in toluene) via syringe. Immediately a change in color from yellow to dark green-black was observed. The reaction mixture was heated under reflux for 12 h, and 6 equiv of allyl bromide (24.9 mmol, 3.0 g, 2.15 mL) was added. After 30 min a brightening of the solution was observed and the reaction mixture was heated to 60 °C overnight. Removal of the solvent and of the excess allyl bromide by evaporation resulted in a pale yellow powder, which was extracted with pentane (3 × 20 mL). The solution was concentrated and stored at room temperature for 24 h and was afterward filtered again. Compound **2** was isolated by removal of the solvent in vacuo as 1.4 g of a yellow powder in 65% yield. Mp: 160 °C. Anal. Calcd for $C_{36}H_{47}N_3$: C, 82.92; H, 9.02; N, 8.06. Found: C, 82.96; H, 8.55; N, 8.03. ^{1}H NMR ($CDCl_3$; δ (*J*, Hz)): 1.13−1.22 (m, 24H, $CHMe_2$), 2.24 (s, 3H, MeC=N), 2.27−2.31 (m, 2H, CH_2), 2.73−2.80 (m, 6H, CH_2 + $CHMe_2$), 4.83−4.89 (m, 2H, CH_2=C), 5.66−5.73 (dq, 1H, CH_2=CH), 7.02−7.12 (m, 2H, H_p aryl), 7.15−7.18 (t, 4H, H_m aryl), 7.92 (t, 1H, $^3J_{HH}$ = 7.7, H_p py), 8.40 (d, 1H, $^3J_{HH}$ = 7.7, H_m py), 8.45 (d, 1H, $^3J_{HH}$ = 7.7, H_m py). ^{13}C{^{1}H} NMR ($CDCl_3$; δ): 17.238 (MeC=N), 22.220 ($CHMe_2$), 22.904 ($CHMe_2$), 23.217 ($CHMe_2$), 23.515 ($CHMe_2$), 28.316 ($CHMe_2$), 29.945 (CH_2), 30.854 (CH_2), 114.699 (CH_2=CH), 122.097 (C_m py), 122.853 (C_m py), 123.006 (C_p aryl), 123.544 (C_m aryl), 123.624 (C_m aryl), 135.487 (C_{quat}), 135.800 (C_{quat}), 137.044 (C_p py), 137.786 (CH=CH_2), 145.515 (C_{quat}), 146.380 (C_{quat}), 154.911 (C_{quat}), 155.089 (C_{quat}), 166.968 (C=N), 168.812 (C=N). IR (cm^{-1}): $\tilde{\nu}$ 3062.3 m, 2960.9 s, 2926.2 s, 2867.1 m, 1633.9 s, 1568.7 m, 1454.8 s, 1435.7 s, 1382.0 m, 1363.7 s, 1325.7 m, 1254.1 m, 1238.0 m, 1191.4 m, 1109.8 s, 1076.8 w, 1058.1 w, 1044.3 w, 994.5 w, 935.5 w, 912.5 m, 820.3 m, 780.3 m, 758.3 s, 689.5 w, 531.5 w. MS (*m*/*z*): 521 (M^+), 506.4 (M^+ − Me), 478.5 (M^+ − allyl).

Synthesis of 2-[1-(2,6-(Diisopropylphenyl)imino)ethyl]-6-[1-(2,6-(diisopropylphenyl)imino)-5-hexenyl]pyridine (3). By using the procedure described above, 1.75 g (79%) of **3** was obtained as a yellow powder with 2 g (4.15 mmol) of 2,6-bis[1-(2,6-(diisopropylphenyl)imino)ethyl]pyridine (**1**), 2.2 mL (4.4 mmol, 1.05 equiv) of lithium diisopropylamide (2 M in toluene) and 1.0 mL (8.3 mmol, 2.0 equiv) of 4-bromo-1-butene. Mp: 150 °C. Anal. Calcd for $C_{37}H_{49}N_3$: C, 82.99; H, 9.16; N, 7.85. Found: C, 82.66; H, 9.27; N, 7.51. ^{1}H NMR ($CDCl_3$; δ (*J*, Hz)): 1.12−1.21 (m, 24H, $CHMe_2$), 1.57−1.62 (m, 2H, CH_2), 1.95−2.00 (m, 2H, CH_2), 2.24 (s, 3H, MeC=N), 2.67−2.71 (m, 2H, CH_2), 2.74−2.80 (m, 4H, $CHMe_2$), 4.81−4.86 (m, 2H, CH_2=CH), 5.59−5.67 (dq, 1H, CH=CH_2), 7.06−7.12 (m, 2H, H_p aryl), 7.15−7.18 (m, 4H, H_m aryl), 7.89 (t, 1H, $^3J_{HH}$ = 8.2, H_p py), 8.40 (d, 1H, $^3J_{HH}$ = 8.2, H_m py), 8.43 (d, 1H, $^3J_{HH}$ = 8.2, H_m py). ^{13}C{^{1}H} NMR ($CDCl_3$; δ): 17.130 (MeC=N), 17.236 (MeC=N), 22.177 ($CHMe_2$), 22.893 ($CHMe_2$), 23.223 ($CHMe_2$), 23.547 ($CHMe_2$), 25.857 (CH_2), 28.301 ($CHMe_2$), 30.045 (CH_2), 34.265 (CH_2), 114.820 (CH_2=CH), 122.080 (C_m py), 122.814 (C_m py), 123.006 (C_p aryl), 123.483 (C_m aryl), 123.628 (C_m aryl), 135.558 (C_{quat}), 135.818 (C_{quat}), 136.997 (C_p py), 137.944 (CH=CH_2), 145.951 (C_{quat}), 146.367 (C_{quat}), 154.645 ($_{quat}$), 155.090 (C_{quat}), 166.991 (C=N), 168.922 (C=N). IR (cm^{-1}): $\tilde{\nu}$ 3062.7 m, 2980.3 s, 2923.1 m, 2867.2 m, 1641.9 s, 1568.4 m, 1455.8 s, 1434.7 m, 1363.6 m, 1325.6 m, 1254.5 w, 1237.5 m, 1193.3 m, 11.09.8 m, 1077.3 w, 994.0 w, 910.6 w, 829.5 w, 768.4 s, 688.1 w. MS (*m*/*z*:) 535.5 (M^+), 481.5 (M^+ − butenyl), 466.5 [M^+ − (butenyl, Me)].

Synthesis of 2-[1-(2,6-(Diisopropylphenyl)imino)ethyl]-6-[1-(2,6-(diisopropylphenyl)imino)-6-heptenyl]pyridine (4). In an analogous manner 1.65 g (72.4%) of **4** could be obtained as a yellow powder from 2 g (4.15 mmol) of 2,6-bis-[1-(2,6-(diisopropylphenyl)imino)ethyl]pyridine, 2.2 mL (4.4 mmol, 1.05 equiv) of lithium diisopropylamide (2 M in toluene), and 1.0 mL (8.3 mmol, 2 equiv) of 5-bromo-1-pentene. Mp: 155 °C. Anal. Calcd for $C_{38}H_{51}N_3$: C, 83.06; H, 9.29; N, 7.65. Found: C, 82.63; H, 9.46; N, 7.42. ^{1}H NMR ($CDCl_3$; δ (*J*, Hz)): 1.12−1.21 (m, 24H, $CHMe_2$), 1.29−1.38 (m, 2H, CH_2), 1.50−1.55 (m, 2H, CH_2), 1.88−1.93 (m, 2H, CH_2), 2.24 (s, 3H, MeC=N), 2.66−2.86 (m, 2H, CH_2), 2.72−2.80 (m, 4H, $CHMe_2$), 4.80−4.84 (m, 2H, CH_2=CH), 5.58−5.68 (dq, 1H, CH=CH_2), 7.06−7.12 (m, 2H, H_p aryl), 7.14−7.18 (m, 4H, H_m aryl), 7.91 (t, 1H, $^3J_{HH}$ = 7.7, H_p py), 8.41 (d, 1H, $^3J_{HH}$ = 7.7, H_m py), 8.48 (d, 1H, $^3J_{HH}$ = 7.7, H_m py). ^{13}C{^{1}H} NMR ($CDCl_3$; δ): 17.232 (MeC=N), 22.188 ($CHMe_2$), 22.897 ($CHMe_2$), 23.224 ($CHMe_2$), 23.537 ($CHMe_2$), 26.055 (CH_2), 28.310 ($CHMe_2$), 29.523 (CH_2), 30.479 (CH_2), 33.393 (CH_2), 114.536 (CH_2=CH), 122.042 (C_m py), 122.797 (C_m py), 123.008 (C_p aryl), 123.452 (C_m aryl), 123.616 (C_m aryl), 135.540 (C_{quat}), 135.806 (C_{quat}), 136.978 (C_p-Py), 138.351 (CH=CH_2), 146.016 (C_{quat}), 146.408 (C_{quat}), 154.680 (C_{quat}), 155.062 (C_{quat}), 166.978 (C=N), 169.492 (C=N). IR (cm^{-1}): $\tilde{\nu}$ 3062.8 m, 2960.7 s, 2927.1 s, 2866.7 s, 1635 s ($\nu_{C=N}$), 1588.6 w, 1568.6 w, 1456.9 s, 1435.2 s, 1382.0 w, 1362.8 s, 1325.4 m, 1254.4 m, 1236.6 m, 1192.5 m, 1109.3 s, 1043.1 w, 994.0 w, 911.2 w, 818.4 m, 765.0 s, 684.7 w, 529.8 w. MS (*m*/*z*): 549.8 (M^+), 534.7 (M^+ − Me), 481.6 (M^+ − pentenyl), 466.5 [M^+ − (pentenyl, Me)].

Synthesis of 2-[1-(2,6-(Diisopropylphenyl)imino)ethyl]-6-[1-(2,6-(diisopropylphenyl)imino)-4-pentenyl]pyridyliron(II) Chloride (5). A 200 mg portion of ligand **2** (0.38 mmol) was dissolved in 20 mL of THF, and 0.95 equiv (72 mg) of $FeCl_2 \cdot 4H_2O$ was added with continuous, vigorous stirring. The blue solution was stirred at room temperature for 20 h. Afterward, compound **5** was precipitated with 30 mL of pentane. The solution was filtered off and the remaining blue solid washed with pentane and toluene and thoroughly dried in vacuo. This synthesis afforded compound **5** as a blue powder in 83% yield (194 mg). Mp: >250 °C dec. Anal. Calcd for $C_{36}H_{47}N_3FeCl_2$: C, 66.69; H, 7.26; N, 6.48. Found: C, 66.21; H, 7.26; N, 6.26. ^{1}H NMR (CD_2Cl_2; δ): −39.5 (s, 3H, MeC=N), −26.5 (br, 2H, $CHMe_2$), −21.7 (br, 2H, $CHMe_2$), −11.4 (s, 1H, H_p aryl), −10.5 (s, 1H, H_p aryl), −9.2 (br, 6H, $CHMe_2$), −6.8 (s, 6H, $CHMe_2$), −6.6 (s, 6H, $CHMe_2$), −5.1 (s, 6H, $CHMe_2$), −4.4 (br, 2H, CH_2), 4.0 (s, 1H, CH=CH_2), 4.8 (s, 1H, CH=CH_2), 6.1 (br, 1H, CH=CH_2), 6.4 (br, 2H, CH_2), 14.0 (s, 2H, H_m aryl), 15.4 (s, 2H, H_m aryl), 79.5 (s, 1H, HPy), 83.2 (s, 1H, HPy), 86.4 (s, 1H, HPy). IR (cm^{-1}): $\tilde{\nu}$ 3062.3 w, 2962.9 s, 2925.8 m, 2867.0 m, 1624.4 w, 1577.1 s, 1465.0 s, 1383.7 m, 1363.1 m, 1325.1 m, 1269.6 m, 1203.9 m, 1186.4 m, 1104.0 m, 1056.9 w, 936.7 m, 816.0 m, 794.5 m, 768.2. MS (*m*/*z*): 647.0 (M^+), 612.1 (M^+ − Cl), 577.0 (M^+ − 2Cl), 522.0 (M^+ − $FeCl_2$).

Synthesis of 2-[1-(2,6-(Diisopropylphenyl(imino)ethyl]-6-[1-(2,6-(diisopropylphenyl)imino)-5-hexenyl]pyridyliron-(II) Chloride (6). With ligand **3** (200 mg; 0.37 mmol) as the

starting material and using a procedure analogous to the one described above, **6** could be obtained as a blue powder in 79% yield (184 mg). Mp: >250 °C dec. Anal. Calcd for $C_{37}H_{49}N_3FeCl_2$: C, 67.10; H, 7.40; N, 6.35. Found: C, 66.85; H, 7.23; N, 5.98. ^{1}H NMR (CD_2Cl_2; δ): −41.2 (s, 3H, MeC═N), −26.5 (br, 2H, $CHMe_2$), −22.3 (br, 2H, $CHMe_2$), −11.5 (s, 1H, H_p aryl), −10.3 (s, 1H, H_p aryl), −9.1 (br, 6H, $CHMe_2$), −6.7 (s, 12H, $CHMe_2$), −5.3 (br, 2H, CH_2), −5.0 (br, 6H, $CHMe_2$), −1.5 (br, 2H, CH_2), 3.0 (s, 2H, CH_2), 5.5 (s, 2H, CH_2═CH), 5.9 (s, 1H, CH═CH_2), 14.0 (s, 2H, H_m aryl), 15.5 (s, 2H, H_m aryl), 79.3 (s, 1H, HPy), 83.6 (s, 1H, HPy), 85.7 (s, 1H, HPy). IR (cm^{-1}): $\tilde{\nu}$ 3061.4 w, 2962.1 s, 2923.1 m, 2866.8 m, 1577.4 s, 1463.6 s, 1383.8 m, 1368.8 m, 1323.8 m, 1264.0 m, 1204.4 m, 1187.9 m, 1103.8 m, 1057.2 w, 989.7 w, 938.0 w, 916.8 m, 810.2 m, 778.7 m. MS (*m*/*z*): 660.8 (M^+), 625.9 (M^+ − Cl), 609.9 [M^+ − (Cl, Me)], 590.1 (M^+ − 2Cl), 536.0 (M^+ − $FeCl_2$).

Synthesis of 2-[1-(2,6-(Diisopropylphenyl)imino)ethyl]-6-[1-(2,6-(diisopropylphenyl)imino)-6-heptenyl]pyridyliron(II) Chloride (7). Starting with ligand **4** (200 mg; 0,36 mmol) and using the procedure described above, compound **7** could be obtained as a blue powder in 75% yield (173 mg). Mp: >250 °C dec. Anal. Calcd for $C_{38}H_{51}N_3FeCl_2$: C, 67.48; H, 7.55; N, 6.22. Found: C, 67.02; H, 7.55; N, 5.96. ^{1}H NMR (CD_2Cl_2; δ): −41.1 (s, 3H, MeC═N), −26.1 (br, 2H, $CHMe_2$), −22.2 (br, 2H, $CHMe_2$), −11.4 (s, 1H, H_p aryl), −10.3 (s, 1H, H_p aryl), −9.1 (br, 6H, $CHMe_2$), −6.6 (s, 12H, $CHMe_2$), −5.3 (br, 2H, CH_2), −4.9 (br, 6H, $CHMe_2$), −1.7 (br, 2H, CH_2), 1.8 (br, 2H, CH_2), 2.3 (s, 2H, CH_2), 5.5 (s, 2H, CH_2═CH), 6.1 (s, 1H, CH═CH_2), 14.0 (s, 2H, H_m aryl), 15.5 (s, 2H, H_m aryl), 79.2 (s, 1H, HPy), 83.4 (s, 1H, HPy), 85.1 (s, 1H, HPy). IR (cm^{-1}): $\tilde{\nu}$ 3062.3 w, 2962.0 s, 2923.1 m, 2866.7 m, 1578.2 s, 1463.9 s, 1389.8 m, 1389.0 m, 1324.8 m, 1272.3 m, 1204.4 m, 1103.7 m, 1057.1 w, 914.4 m, 809.9 m, 777.4 m. MS (*m*/*z*): 675.7 (M^+), 640.7 (M^+ − Cl), 625.6 [M^+ − (Cl, Me)], 605.6 (M^+ − 2Cl), 550.7 (M^+ − $FeCl_2$).

Self-Immobilization of Compounds 5−7 on Silica (8−10). A 15 mg portion (0.0225 mmol) of **5**, **6**, or **7** was dissolved in 20 mL of absolute toluene and cooled to 0 °C. On addition of 100 equiv of MMAO the color of the solution turned from deep brown to green-brown. Dry and oxygen-free ethylene was slowly bubbled through the solution, until the solution turned opaque and small quantities of polymer began to precipitate. The reaction vessel was transferred into a glovebox and the polymer separated via centrifugation, thoroughly washed with toluene and hexane, and dried in vacuo. The obtained self-immobilized catalyst was used in olefin polymerization.

For NMR experiments the self-immobilized catalyst was hydrolyzed with methanol and the resulting polymer thoroughly washed with methanol, THF, toluene and hexane and dried in vacuo.

^{1}H NMR ($C_2D_2Cl_4$, 390 K; δ): 0.87 (s, polymer CH_3), 1.1−1.9 (s, polymer CH_2), 1.1−1.9 (s, $CHMe_2$), 1.1−1.9 (s, CH_2), 1.1−1.9 (s, CH_2), 1.1−1.9 (s, CH_2), 2.22 (s, MeC═N), 2.76 (s, $CHMe_2$), 7.07−7.24 (m, H aryl), 7.91 (t, H py), 8.31−8.52 (m, H py). ^{13}C{^{1}H} NMR ($C_2D_2Cl_4$, 390 K; δ): 16.828 (MeC═N), 21.117−25.013 (polymer CH_3), 21.117−25.013 ($CHMe_2$), 21.117−25.013 ($CHMe_2$), 21.117−25.013 ($CHMe_2$), 21.117−25.013 ($CHMe_2$), 25.980 (CH_2), 28.532 ($CHMe_2$), 28.885 (CH_2), 30.577 (CH_2), 29.655−34.234 (polymer CH_2), 35.091 (CH_2), 121.042−125.142 (C py, C aryl), 133.841−139.221 (C py, C aryl), 144.992−147.002 (C aryl), 153.553−155.996 (C aryl), 167.287 (C═N).

Modification of the Silica Support. To a suspension of 2 g of dehydroxylated silica (500 °C, 15 h, 2×10^{-4} mbar) in 20 mL of hexane was added 0.8 g (6 mmol) of tetramethyldisilazane dropwise at room temperature. The resulting suspension was heated to 85 °C for 4 h. The solid was separated via filtration and washed three times with 20 mL of hexane. The support was dried in vacuo at room temperature for 30 h. The carbon content was determined as high as 1.98%. BET surface: 202 m^2/g. Pore volume (BJH, cumulative, desorption, 17−1000 Å): 1.59 cm^3/g.

Immobilization of Compounds 5−7 on Silica (8−10). A 100 mg portion (0.15 mmol) of **5**, **6**, or **7** was combined with 500 mg of modified silica in a Schlenk tube. On addition of 6 mL of absolute THF and 0.1 mL of the Karstedt catalyst (3−3.5 wt % Pt in xylene), the reaction mixture was stirred at 55 °C for 4 days. After that time, the resulting solid was separated via filtration, thoroughly washed with toluene, and dried in vacuo. The Fe content on the silica was determined to be 1.15 wt % Fe for precatalyst **8**, 1.10 wt % Fe for precatalyst **9**, and 0.99 wt % Fe for precatalyst **10**.

Ethene and Propene Polymerization and Analytical Procedures. Polymerization Procedures for Homogeneous and Heterogeneous [Bis(imino)pyridyl]iron(II) Precatalyst. A 0.5 L Büchi glass autoclave, equipped with a pressflow gas controller, was filled with approximately 230 mL of dry and oxygen-free toluene and the appropriate amount of MMAO (10% in heptane; Al:Fe = 1000). The autoclave was pressurized with ethene or propene and thermostated to the desired reaction temperature. The desired amount of precatalyst was dissolved or suspended in dry and oxygen-free toluene, the precatalyst was transferred into the injection system via a syringe or a cannula, the injection system was closed, the solution/suspension was injected into the autoclave, and the injection system was washed with an additional 5 mL of toluene. The pressure was kept constant during the polymerization, and the amount of ethene or propene consumed by the catalyst during the reaction was measured. The polymerization was quenched after 1 h by adding 10 mL of methanol, and the resulting polymer suspension was poured into 250 mL of methanol/HCl (3:1) to precipitate the polymer and stirred for 16 h. After filtration the polymer was dried at 60 °C in vacuo.

Results

Syntheses of Alkene-Functionalized Ligands. With the 2,6-bis[1-(2,6-(diisopropylphenyl)imino)ethyl]-pyridine ligand (**1**) reported by Brookhart and Gibson[1,2] as the starting material, the functionalization is achieved by deprotonation of the bis(imino)pyridine ligand with lithium diisopropylamide. Immediately the yellow solution turns dark green, almost black. After the mixture is kept under reflux for 12 h, addition of an excess of allyl bromide to the stirred solution leads to the formation of the allyl-modified ligand **2** within a reaction time of 1 day (Scheme 1).

When the reaction is finished, the color of the solution returns to yellow. In analogous manner the butenyl- (**3**) and pentenyl-modified (**4**) ligands can be prepared in good yields. The reaction time of the nucleophilic substitution depends on the alkenyl bromide and increases with increasing chain length, because of the greater steric hindrance of the longer chains, but using a greater excess of the bromoalkene accelerates the reaction.

The modified ligands show an increased solubility compared with **1**, especially in pentane, which is used to separate the product from the unreacted educt. The pentenyl-substituted bis(imino)pyridyl ligand is the most soluble one, followed by the butenyl- and the allyl-modified bis(imino)pyridyl ligands.

After the preparation of the ligands, the iron(II) complexes are synthesized according to published methods[1,2] by addition of $FeCl_2 \cdot 4H_2O$ to a stirred solution of the ligands **2**−**4** in THF (Scheme 2). The resulting deep blue iron complexes **5**−**7** can be precipitated with pentane.

Scheme 1. Preparation of the Alkenyl-Functionalized 2,6-Bis[1-(2,6-(diisopropylphenyl)imino)ethyl]pyridyl Ligands 2−4[a]

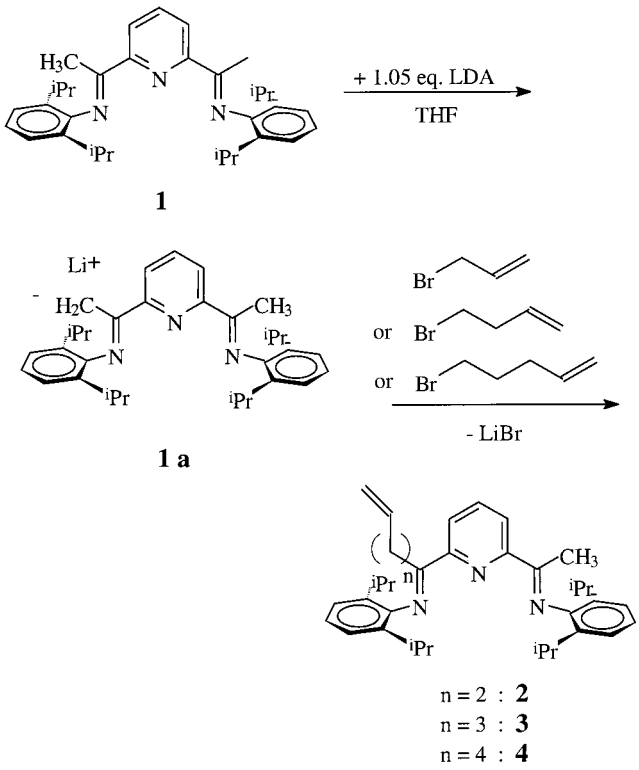

[a] LDA = lithium diisopropylamide.

Scheme 2. Preparation of the Alkenyl-Functionalized [Bis(imino)pyridyl]iron(II) Complexes 5−7

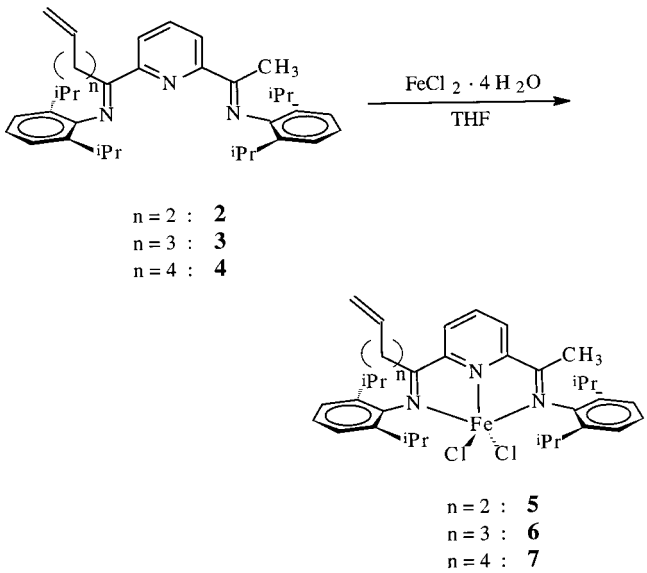

Polymerization. The precatalysts were activated by MMAO and used in the polymerization of ethene and propene. As shown in Table 1 and Scheme 3, all precatalysts exhibit an extremely high ethene polymerization activity of 24 000−107 000 kg of PE/((mol of Fe) h bar) (at 0 °C). Precatalyst **5** shows the lowest polymerization activity, which increases for **6** and **7.** All precatalysts show a strong temperature dependence of their activity and of the average lifetime during ethene polymerization, decreasing from 0 to 80 °C. Whereas **6** and **7** are strongly affected by increasing temperature (decrease of activity from 105 000 to 10 100 kg of PE/((mol of Fe) h bar) and from 107 000 to 10 800 kg of PE/((mol of Fe) h bar), respectively), only precatalyst **5** shows more constant, but considerably lower, average activities at temperatures of 0−60 °C.

Table 1. Results of Ethene Polymerization Runs with Precatalysts 5−7[a]

		activity[b]		
precatalyst	*T* (°C)	after 5 min	after 45 min	average
5	0	4.0×10^4	1.8×10^4	2.40×10^4
	20	5.3×10^4	7.7×10^3	2.14×10^4
	40	8.5×10^4	0	2.08×10^4
	60	9.2×10^4	0	1.15×10^4
	80	2.1×10^4	0	3.38×10^3
6	0	4.5×10^5	2.6×10^4	1.05×10^5
	20	3.6×10^5	7.2×10^3	7.72×10^4
	40	3.5×10^5	0	6.90×10^4
	60	2.5×10^5	0	2.49×10^4
	80	8.1×10^4	0	1.01×10^4
7	0	2.8×10^5	4.7×10^4	1.07×10^5
	20	2.0×10^5	1.4×10^4	5.98×10^4
	40	2.2×10^5	0	4.13×10^4
	60	2.1×10^5	0	3.33×10^4
	80	6.9×10^4	0	1.08×10^4

[a] Reaction conditions: 2.0 bar of ethene pressure; toluene as solvent; cocatalyst MMAO (Al:Fe = 1000); reaction time 1 h. [b] In units of kg of PE/((mol of Fe) h bar).

Scheme 3. Self-Immobilization of Alkenyl-Functionalized [Bis(imino)pyridyl]iron(II) Complexes

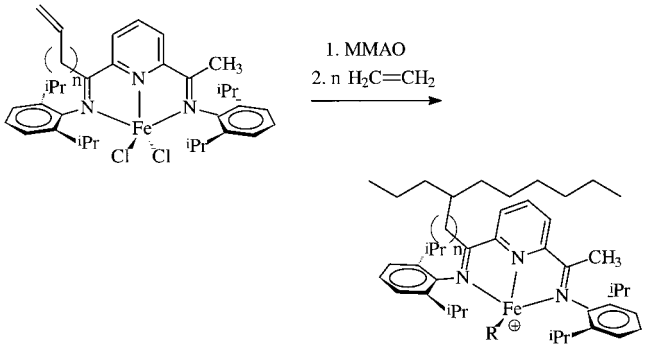

The catalysts are rapidly deactivated during the polymerization procedures at higher temperatures (Tables 1 and 2).

At temperatures above 20 °C, a complete deactivation of the catalysts can be observed within 40 min and even faster times (within 20−30 min) are obtained at temperatures above 60 °C. The rapid deactivation of the catalysts may also originate from the self-immobilization of the catalysts via copolymerization of the alkenyl moiety of the [bis(imino)pyridyl]iron(II) catalysts with the olefin during the polymerization experiment. Figure 1 demonstrates the dependence of the average activities of precatalysts **5**−**7** on the polymerization temperature.

Due to faster deactivation of the catalyst at elevated temperatures, the calculated average polymerization activities of the catalysts **5**−**7** are significantly lower than at low temperatures, although the activities at the beginning of the polymerization are comparable at all applied polymerization temperatures.

The obtained polymers were analyzed by high-temperature GPC and NMR.

Table 2. Results of Ethene Polymerization Runs with Precatalysts 5−7[a]

precatalyst	*T* (°C)	amt of catalyst used (μmol)	amt of polymer obtained (g)
5	0	0.617	26.73
	20	0.617	24.56
	40	0.617	22.12
	60	0.922	21.89
	80	1.543	10.01
6	0	0.227	4.65
	20	0.604	81.83
	40	0.302	37.11
	60	0.227	9.45
	80	0.756	13.11
7	0	0.355	0.54
	20	0.296	28.59
	40	0.296	22.05
	60	0.296	17.13
	80	0.740	13.99

[a] Reaction conditions: 2.0 bar of ethene pressure; toluene as solvent; cocatalyst MMAO (Al:Fe = 1000); reaction time 1 h.

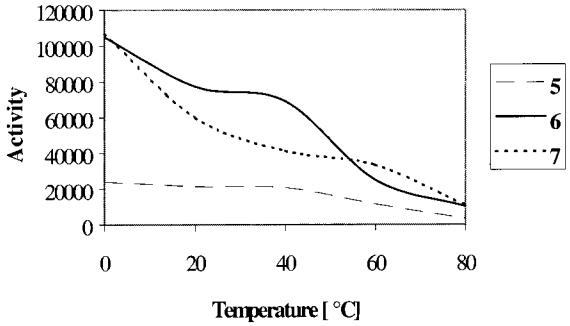

Figure 1. Dependence of the polymerization activity of precatalysts **5**−**7** on polymerization temperature. The activity is given in units of kg of PE/((mol of Fe) h bar).

As Table 3 clearly shows, there is a strong dependence of the molecular weight of the produced polymers on the polymerization temperatures. At low polymerization temperatures the molecular weight distribution exhibits a significant bimodality, which decreases toward higher polymerization temperatures. The high-molecular-weight fraction of the polymer, which seems to be predominant for the polymer produced at 0 °C, disappears at temperatures above 40 °C (at 20 °C only traces of the high-molecular-weight fraction can be detected). In addition, the low-molecular-weight fraction shifts toward even lower molecular weights when the polymerization temperature is increased (approximately 40 000 at 0 °C, approximately 2000 at 80 °C). At intermediate temperatures the molecular weight distribution broadens due to the coincidence of the lower and higher molecular weight fractions (Figure 2).

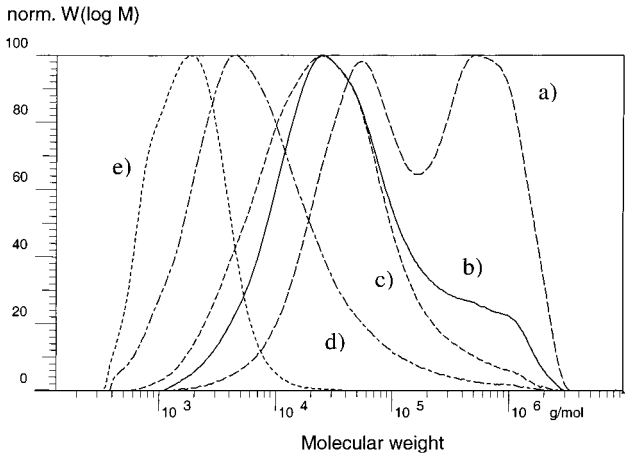

Figure 2. Typical molecular weight distribution of the polymers obtained using precatalyst **6** at different polymerization temperatures: (a) 0 °C; (b) 20 °C; (c) 40 °C; (d) 60 °C; (e) 80 °C. The molecular weight distributions of the polymers obtained by the precatalysts **5** and **7** are analogous.

Although the produced polymers are very similar in molecular weights, polydispersities, and molecular weight distributions, it can be observed that the alkenyl-functionalized catalyst with the shortest spacer moiety produces the highest molecular weights of the polymers, whereas an increase of spacer length decreases the molecular weights of the produced polymers slightly.

As the NMR spectra clearly show, the catalysts succeed in producing linear polyethylene at low and intermediate temperatures up to 40 °C, as predominantly peaks originating from CH_2 groups can be detected at 30.1 ppm in ^{13}C NMR and 1.30 ppm in ^{1}H NMR, respectively. Peaks originating from terminal methyl groups or unsaturated terminal groups are extremely small and confirm the high selectivity of the [bis(imino)pyridyl]iron(II) catalysts for linear polymers and the high molecular weights of the produced polymers.

For higher polymerization temperatures of 60 °C and above additional peaks for terminal methyl groups and

Table 3. Data for the Polymers Produced by Precatalysts 5−7

precatalyst	*T* (°C)	mol wt distribn[a]	M_w	M_n	*D*
5	0	B (40%/60%)	$7.90 \times 10^5/7.82 \times 10^4$	$5.54 \times 10^5 / 3.70 \times 10^4$	1.42/2.11
	20	B (15%/85%)	$6.28 \times 10^5/5.54 \times 10^4$	$3.41 \times 10^5/2.65 \times 10^4$	1.84/2.09
	40	B (5%/95%)	$7.73 \times 10^4/3.88 \times 10^4$	$2.19 \times 10^4/2.78 \times 10^3$	3.53/1.39
	60	M	3.53×10^4	$6.05 \cdot 10^3$	5.84
	80		3.34×10^3	1.64×10^3	2.03
6	0	B (50%/50%)	$7.39 \times 10^5/5.87 \times 10^4$	$4.72 \times 10^5/2.91 \times 10^4$	1.56/2.02
	20	B (12%/88%)	$7.57 \times 10^5/5.66 \times 10^4$	$5.96 \times 10^5/1.70 \times 10^4$	1.27/3.33
	40	B (2%/97%)	$7.61 \times 10^5/4.00 \times 10^4$	$6.68 \times 10^5/9.46 \times 10^3$	1.14/4.23
	60	M	2.57×10^4	3.71×10^3	6.92
	80	M	2.29×10^3	1.41×10^3	1.63
7	0	B (53%/47%)	$6.14 \times 10^5/4.01 \times 10^4$	$3.64 \times 10^5/1.94 \times 10^4$	1.69/2.07
	20	B (21%/79%)	$7.16 \times 10^5/4.55 \times 10^4$	$5.04 \times 10^5/1.50 \times 10^4$	1.42/3.04
	40	B (4%/96%)	$6.78 \times 10^5/3.25 \times 10^4$	$5.32 \times 10^4/8.83 \times 10^3$	1.27/7.68
	60	M	1.15×10^4	2.77×10^3	4.17
	80	M	2.96×10^3	1.66×10^3	1.78

[a] Legend: B, bimodal; M, monomodal. Results from GPC at 135 °C.

terminal alkenyl groups can be observed in ^{13}C and ^{1}H NMR. The signal for the terminal methyl groups can be found at 22.85 ppm in ^{13}C NMR and at 0.87 ppm in ^{1}H NMR. Signals for the unsaturated groups can be detected at 114.38 and 137.61 ppm in ^{13}C NMR and at 4.97 and 5.77 ppm in ^{1}H NMR.

These observations give rise to the assumption that the chain termination at higher temperatures predominantly occurs through β-H transfer, resulting in alkenyl-terminated polymer chains, whereas at low polymerization temperatures no indication for alkenyl-terminated polymer chains could be found.

Self-Immobilization. For self-immobilization the catalysts **5**−**7** are activated with MMAO and ethylene is bubbled through the solution for a short period of time: e.g., 5 min. The polymeric catalysts can be isolated via filtration and, after extensive workup to separate the homogeneous catalyst, used in ethylene polymerization, giving considerably lower activity than the monomeric species.

The incorporation of the catalyst into the polymer chain can be recognized by the green brownish color of the polymer, which spontaneously disappears on exposure to air and moisture.

Due to the air and temperature sensitivity of activtated [bis(imino)pyridyl]iron(II) compounds, an examination of the incorporation of the activated alkenyl-functionalized [bis(imino)pyridyl]iron complexes into the polymer chain can best be achieved by an hydrolysis of the self-immobilized activated catalyst and an NMR examination of the obtained polymer, which contains the self-immobilized catalyst ligand framework.

As the NMR data clearly show, nearly identical signals are obtained for the homogeneous bis(imino)-pyridine ligand and the polymer-incorporated ligand framework after hydrolysis of the active catalyst. Although the signals of the bis(imino)pyridine ligand are small compared to the signals obtained by the CH_2 and CH_3 groups of the polymer chain and are partially overlaid by the polymer signals, the incorporation of the ligand moiety can be demonstrated by ^{1}H and ^{13}C NMR.

As experiments showed, the activated [bis(imino)-pyridyl]iron(II) complexes are not stable in the absence of olefins and decompose rather quickly at room temperature. Therefore, the polymerization activity of the polymeric species, obtained by the self-immobilization of the monomeric alkenyl-functionalized [bis(imino)-pyridyl]iron(II) compounds, decreases rapidly when the polymeric catalysts are isolated and especially when they are stored over a longer period of time.

In agreement with data found for the monomeric species **5**−**7**, the self-immobilized catalysts exhibit higher polymerization activities, longer catalyst lifetimes, and higher overall polymer molecular weights at low temperatures than at higher (>40 °C) temperatures.

To rule out the influence of the Karstedt catalyst, control experiments have been started in order to find polymerization activity by adding to a solution of Karstedt catalyst various amounts of MMAO. Neither this reaction mixture nor addition of iron(II) chloride or iron(III) chloride showed any ethene polymerization activity.

Immobilization on Silica. An easy access to supported polymerization catalysts is the coupling of the

Scheme 4. Immobilization of the Alkenyl-Functionalized [Bis(imino)pyridyl]iron(II) Complexes on a Modified Silica Surface

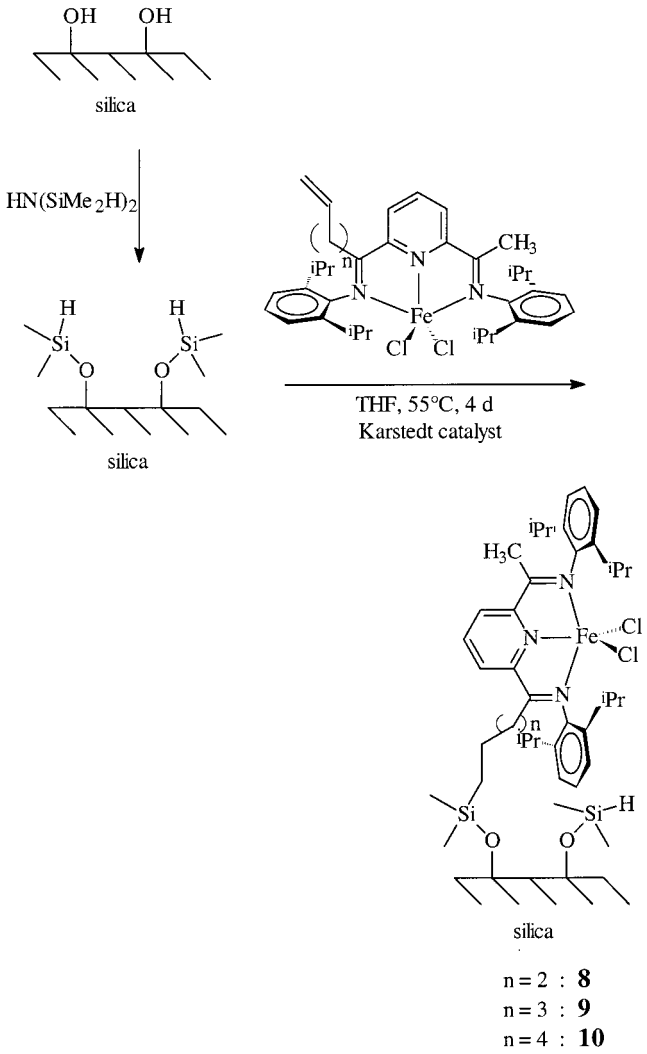

alkene-functionalized [bis(imino)pyridyl]iron(II) complexes with an SiR_2H-modified surface via hydrosilation of the alkenyl moiety of the homogeneous precatalyst with Si−H groups of the modified silica surface. Therefore, in a first step, the Si−OH groups of the dehydroxylated support have to be functionalized with Si−H surface groups. This transformation can be performed by treating the support with tetramethyldisilazane (TMDS), which nearly selectively converts free (and to a minor extend bonded) surface OH groups into $OSiMe_2H$ groups.

In a second step, the alkenyl-functionalized [bis-(imino)pyridyl]iron(II) complexes can be reacted with the surface Si−H groups with the use of Karstedt catalyst as a coupling reagent (Scheme 4) to yield the covalently tethered [bis(imino)pyridyl]iron(II) complexes. To ensure the intended formation of a covalent bond between the alkenyl-functionalized homogeneous [bis(imino)pyridyl]iron(II) complexes and the SiR_2H-modified silica surface via hydrosilation, infrared spectroscopy has been applied (Figure 3).

To monitor the covalent immobilization of the catalysts, IR spectra of the $SiMe_2H$-modified support (Figure 3, spectrum A) and the catalysts (Figure 3, spectra B−D) have been recorded. The decrease of the intensity of the

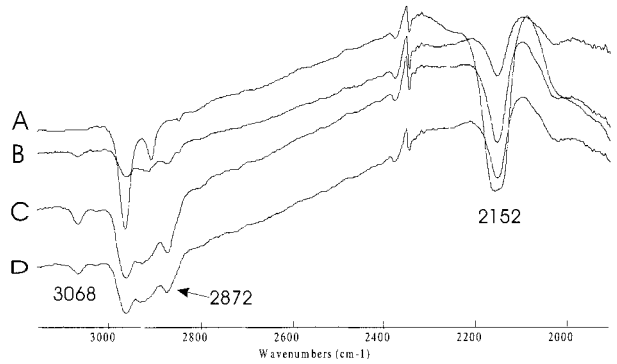

Figure 3. Infrared spectra of the hetergeneous precatalysts: (A) $Si(Me)_2H$-modified support; (B) anchored catalyst **8**; (C) anchored catalyst **9**; (D) anchored catalyst **10**.

Table 4. BET/BJH Data and Fe Content of Catalysts 8−10

	heterogeneous precatalyst			support + Karstedt catalyst
	8	**9**	**10**	
surface BET ($m^2\ g^{-1}$)	178	189	178	198
pore vol ($cm^3\ g^{-1}$)[a]	1.1	1.3	1.1	1.5
Fe (wt %)	1.15	1.10	0.99	0

[a] BJH, desorption, cummulative, 17−1000 Å.

Si−H band (2152 cm^{-1}) after the immobilization clearly shows the formation of a covalent bond between the alkenyl-functionalized [bis(imino)pyridyl]iron(II) complex and the $SiMe_2H$-modified surface. The appearance of aromatic bands around 3068 cm^{-1} and new aliphatic bands around 2870 cm^{-1} in the catalyst spectra (Figure 3, spectra B−D) confirms the presence of aromatic and aliphatic moieties of the supported catalyst. To rule out any influence of the Karstedt catalyst on polymerization results, control experiments under identical hydrosilation conditions using the modified support and various amounts of hydrosilation catalyst have shown nearly no difference concerning the Si−H band at 2152 cm^{-1} compared with spectrum A. This result leads to the assumption that practically no covalent bonding between the Karstedt catalyst and the modified support occurs.

As presented in Table 4, the BET surfaces of the heterogenized precatalysts **8−10** decrease by approximately 10% during the immobilization of the [bis(imino)-pyridyl]iron(II) complex and a decrease of the pore volume from 1.6 $cm^3\ g^{-1}$ to around 1.2 $cm^3\ g^{-1}$ can be observed. Both the IR data and the BET data give rise to the assumption that the covalent anchoring of the alkenyl functionalized iron(II) complexes **5−7** was successful and that the catalysts are anchored not only on the outer surface but also in the pores of the support. In contrast, the BET and BJH numbers of the control experiments (support + Karstedt catalyst) are close to the results obtained from modified support (Table 4). Therefore, we suggest no or just a very small amount of anchored Karstedt catalyst.

Elemental analysis shows that the percent load of iron on the silica (Table 4) varies between 0.99 wt % for catalyst **10** and 1.15 wt % for the allyl-functionalized catalyst **8**. This roughly corresponds to the size of the Si−H band in the IR spectra, as the size of the signal of the Si−H moiety decreases most in the case of the heterogeneous precatalyst **8**, which exhibits the highest loading of iron. Elemental analysis gave no evidence of self-immobilization of the Pt hydosilation catalyst on the support. Also, control experiments have been started wherein various amounts of the Karstedt catalyst and the modified silica were mixed together under identical hydrosilation conditions. Neither a suspension of this mixture nor addition of MMAO, iron(II) chloride, or iron-(III) chloride showed any catalytic activity toward polymerization of ethene.

Table 5. Results of Ethene Polymerization Runs with Immobilized Catalysts 8−10[a]

		activity[b]		
precatalyst	t (°C)	after 5 min	after 45 min	average
8	0	2.8×10^4	2.7×10^3	6.61×10^3
	20	2.4×10^4	1.7×10^3	4.53×10^3
	40	3.0×10^4	1.4×10^3	4.33×10^3
	60	2.0×10^4	400	2.17×10^3
		9.0×10^3		500
9	0	3.7×10^4	5.1×10^3	9.31×10^3
	20	2.9×10^4	2.6×10^3	7.52×10^3
	40	2.8×10^4	1.5×10^3	4.53×10^3
	60	3.8×10^4	700	3.77×10^3
	80	8.2×10^3	40	500
10	0	3.3×10^4	4.6×10^3	9.71×10^3
	20	2.4×10^4	2.8×10^3	7.00×10^3
	40	2.6×10^4	1.2×10^3	4.05×10^3
	60	2.4×10^4	500	3.17×10^3
	80	9.5×10^3	200	900

[a] Reaction conditions: 2.0 bar of ethene pressure; toluene as solvent; cocatalyst MMAO (Al:Fe = 1000); reaction time 1 h. [b] In units of kg of PE/((mol of Fe) h bar).

Table 6. Results of Ethene Polymerization Runs with Immobilized Catalysts 8−10[a]

precatalyst	T (°C)	amt of catalyst used (μmol of Fe)	amt of polymer obtained (g)
5	0	4.180	51.23
	20	4.283	33.87
	40	4.777	38.19
	60	4.345	16.14
	80	4.819	3.01
6	0	3.920	59.98
	20	4.373	61.23
	40	4.235	35.51
	60	4.136	28.67
	80	8.529	6.20
7	0	3.394	59.17
	20	4.325	56.15
	40	3.989	27.36
	60	4.308	23.44
	80	4.148	6.31

[a] Reaction conditions: 2.0 bar of ethene pressure; toluene as solvent; cocatalyst MMAO (Al:Fe = 1000); reaction time 1 h.

Polymerization Results. As shown in Tables 5 and 6 and Figure 4, all heterogenized precatalysts show a good polymerization activity in the range of 10^3-10^4 kg of PE/((mol of Fe) h bar). Analogous to the homogeneous precatalysts, the compound with the shortest alkenyl moiety, the allyl-functionalized compound **8** exhibits the lowest activity, whereas the activity increases with increasing length of the alkenyl chain (compounds **9** and **10** exhibit a higher activity). The activities decrease at higher temperatures for all heterogenized precatalysts, reaching a minimum activity of only 500 kg of PE/((mol of Fe) h bar) at high temperatures of 80 °C. However, in comparison to the homogeneous precatalysts **5−7,** which provide no activity after 45 min at temperatures

Table 7. Data for the Polymers Produced by 8−10

precatalyst	*T* (°C)	mol wt distribn	M_w	M_n	*D*
8	0	B (74%/26%)	$8.97 \times 10^5/4.45 \times 10^4$	$3.96 \times 10^5/ 2.63 \times 10^4$	2.27/1.69
	20	B (75%/15%)	$7.34 \times 10^5/1.27 \times 10^4$	$2.31 \times 10^5/7.65 \times 10^3$	3.18/1.66
	40	B (79%/21%)	$6.95 \times 10^5/4.75 \times 10^3$	$1.13 \times 10^5/2.51 \times 10^3$	6.13/1.89
	60	B (84%/16%)	$5.10 \times 10^5/1.72 \times 10^3$	$5.99 \times 10^4/1.04 \times 10^3$	8.52/1.65
	80	B (9%/91%)	$4.17 \times 10^4/690$	$2.76 \times 10^4/570$	1.51/1.21
9	0	B (72%/28%)	$8.11 \times 10^5/1.81 \times 10^4$	$3.01 \times 10^5/8.37 \times 10^3$	2.69/2.16
	20	B (78%/22%)	$7.36 \times 10^5/8.42 \times 10^3$	$2.17 \times 10^5/4.66 \times 10^3$	3.40/1.81
	40	B (82%/18%)	$6.79 \times 10^5/2.87 \times 10^3$	$1.05 \times 10^5/1.43 \times 10^3$	6.44/2.01
	60	B (84%/16%)	$4.49 \times 10^5/1.61 \times 10^3$	$4.64 \times 10^5 / 1.01 \times 10^3$	9.59/1.59
	80	B (8%/92%)	$3.41 \times 10^4/600$	$2.35 \times 10^4/520$	1.45/1.15
10	0	B (70%/30%)	$8.77 \times 10^5/1.78 \times 10^4$	$3.10 \times 10^5/9.19 \times 10^3$	2.76/1.94
	20	B (78%/22%)	$6.75 \times 10^5/8.88 \times 10^3$	$2.16 \times 10^5/4.76 \times 10^3$	3.13/1.87
	40	B (82%/18%)	$4.44 \times 10^5/2.83 \cdot 10^3$	$7.75 \times 10^4/1.46 \times 10^3$	5.73/1.94
	60	B (84%/16%)	$4.21 \times 10^5/1.59 \times 10^3$	$4.51 \times 10^4/930$	9.33/1.71
	80	B (8%/92%)	$2.35 \times 10^4/600$	$1.60 \times 10^4/500$	1.47/1.20

higher than 20 °C, the heterogeneous precatalysts exhibit higher activities at elevated temperatures. Precatalyst **8** even shows good activity at 60 °C and remains active after 45 min; precatalysts **9** and **10** exhibit activity after 45 min at even higher temperatures of 80 °C.

Although the average lifetimes of the heterogeneous precatalysts are higher than those of the homogeneous precatalysts, a rise of polymerization temperature strongly reduces the overall lifetimes of all heterogeneous precatalysts and therefore the average polymerization activity of the catalysts. A possible reason for the slower deactivation of the heterogeneous catalyst might be the impossibility of a deactivation of the alkenyl-substituted homogeneous catalyst via self-immobilization, as the alkenyl moiety is covalently bonded to the surface and therefore no longer available for a copolymerization with olefins, which, as experiments showed,[9] partially reduces polymerization activity during the polymerization.

The obtained polymers were analyzed by high-temperature GPC (Table 7, Figure 5) and NMR.

The polymers produced by the heterogeneous precatalysts **8**−**10** are substantially different from those produced by the homogeneous precatalysts **5**−**7**. As can be seen in Table 7 and Figure 5, the polymers obtained with the precatalysts **8**−**10** are of bimodal molecular weight distribution, but unlike the polymers produced by **5**−**7**, the total molecular weight is dominated by the high molecular fraction of the polymer with a molecular mass of approximately 10^5-10^6 g/mol (at temperatures of 0−40 °C). Only a small quantity of the polymer shows a lower molecular mass of approximately 10^3-10^4 g/mol (the polymers produced by the homogeneous precatalysts were dominated by low molecular weights, and the high-molecular-weight fraction completely disappeared at polymerization temperatures >20 °C). In accordance with the polymers produced by **5**−**7**, the molecular weights slightly shift toward lower values, when the polymerization temperature is increased from 0 to 60 °C, and shift very drastically (to a molecular weight of 10^2-10^3) when the temperature is further increased to 80 °C. In addition, the molecular weight distribution becomes nearly monomodal at higher temperatures, but the transition from mono- to bimodal distribution only occurs at very high polymerization temperatures (monomodal molecular weight distributions are obtained at temperatures >40 °C for the homogeneous catalysts and >80 °C for the heterogeneous [bis(imino)pyridyl]iron(II) catalysts).

The highest molecular weights are obtained with precatalyst **8**, which has the shortest alkenyl moiety. An increase of chain length of the alkenyl moiety decreases the molecular weight of the produced polymers slightly, so that the lowest molecular weights are obtained by using the heterogeneous precatalyst **10**. This tendency becomes more obvious when the polymerization is conducted at higher temperatures, whereas the polymers produced by the heterogeneous **8**−**10** at low temperatures are nearly identical.

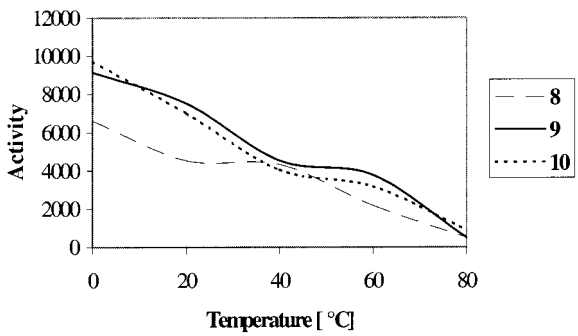

Figure 4. Dependence of the polymerization activity of precatalysts **8**−**10** on polymerization temperature. The activity is given in units of kg of PE/((mol of Fe) h bar).

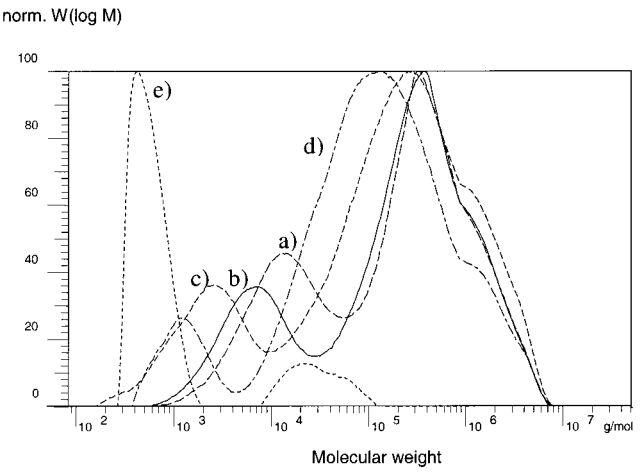

Figure 5. Dependence of the molecular weight of polymers obtained at different temperatures: (a) 0 °C; (b) 20 °C; (c) 40 °C; (d) 60 °C; (e) 80 °C. The molecular weight distributions of the polymers obtained by precatalysts **8**−**10** are analogous.

NMR experiments showed that, in contrast to the homogeneous catalysts, no signals for unsaturated terminal groups could be found in ^{13}C and ^{1}H NMR. Even at higher temperatures no signals for alkenyl groups were detected in ^{13}C and ^{1}H NMR.

Analogous to the case for the homogeneous catalysts, larger signals for terminal methyl groups can be detected at higher temperatures, a fact which correlates well with the lower molecular weights of the polymers produced.

All three catalysts show good activities at high temperatures, even in contrast to the unsupported systems **5**−**7**, which provide no activity after 45 min at temperatures higher than 20 °C. Catalyst **8** shows good activity in the beginning at 60 °C and remains active after 45 min. At 80 °C catalysts **9** and **10** are still active after 45 min. In general, the activities of the supported catalysts are approximately one order of magnitude lower than those of their homogeneous counterparts. In case of the homogeneous precatalysts the variation of the spacer length results in an increase of activity from the allyl-modified catalyst (**5**) to the butenyl- (**6**) or pentenyl-modified catalyst (**7**). The same trend is observed for the supported catalysts **8**−**10**.

For all three supported catalysts no reactor fouling was observed during the whole polymerization process at all polymerization conditions, in contrast to the case for the homogeneous precatalysts **5**−**7**.

Propene polymerization experiments with the homogeneous alkenyl-functionalized [bis(imino)pyridyl]iron(II) catalysts only gave very low starting activities and a complete inactivity of the catalysts after a few minutes of polymerization. Analogous to the ethene polymerization, a higher polymerization activity can be obtained when the polymerization is conducted at very low temperatures, whereas no activity can be detected at polymerization temperatures above 20 °C.

The heterogeneous catalysts failed to show any propene polymerization activity, so that no activity could be detected for any polymerization conditions.

(9) Wieczorek, K.; Puchta, G. T.; Herrmann, W. A. Unpublished results.

Conclusions

The presented modification of ligand **1** is a straightforward approach to alkenyl-functionalized [bis(imino)pyridyl]iron(II) complexes. The peripheral alkenyl moiety allows a variety of useful heterogenization reactions. They include the self-immobilization of the alkenyl-functionalized [bis(imino)pyridyl]iron(II) catalysts and the immobilization on a $SiMe_2H$-modified silica surface via hydrosilation. The covalent bonding to the $SiMe_2H$-modified silica support can be monitored by IR spectroscopy.

The immobilization of the modified [bis(imino)pyridyl]-iron(II) complexes **5**−**7** via hydrosilation results in highly active and temperature-stable catalyst precursors and can be activated with MAO and MMAO. As an important advantage they lack any reactor fouling. As further examination showed, the modification with butenyl or pentenyl groups is more favorable than allyl spacers, at least with regard to catalyst activity.

Acknowledgment. We are grateful to our co-worker A. Osterauer for experimental support and Mr. M. Barth for analytical support. Dr. H. W. Görlitzer is thanked for helpful discussions. This work was generously supported by the Deutsche Forschungsgemeinschaft and the Bayerische Forschungsverbund Katalyse FORKAT.

OM000939T